# Influence of Building Parameters on the Dynamic Mechanical Properties of Polycarbonate Fused Deposition Modeling Parts

Miquel Domingo-Espin,[1] Salvador Borros,[2] Nuria Agullo,[2]
Andres-Amador Garcia-Granada,[1] and Guillermo Reyes[1]

## Abstract

*Fused deposition modeling (FDM) is one of the most important additive manufacturing technologies nowadays. However, there is a need to get more insight in the relationship between the process parameters and the final performance. Several studies have already identified some of these relationships, considering only the mechanical behavior of uniaxial tensile specimen under static loading. Yet, FDM technology is also designed to produce final parts that might be used in machinery or transportation applications. In such cases, dynamic loading is the most common situation and should be considered. The present article focuses on understanding the influence of three process parameters (nozzle diameter, number of contours, and raster-to-raster air gap) on the mechanical behavior under dynamic loading at specified conditions. A dynamic mechanical analysis apparatus has been used to characterize the polycarbonate mechanical behavior. On the other hand, a Taguchi approach and an analysis of variance have been used in order to quantify the influence of the parameters on such mechanical behavior.*

## Introduction

Fused deposition modeling (FDM) is an additive manufacturing technology that consists of building parts depositing the material by layers. Each layer of material is set down using a heated thermoplastic filament and pushed through a nozzle onto a substrate. The nozzle moves following a previously determined track to fulfill a specific area enclosed in contours for each layer. Once the layer is completed, the substrate is lowered to build a new one on top.

The selection of the optimal building factors for FDM requires a multiparametric strategy. The position of the part in the building volume and the nozzle diameter must be chosen for any given material. Other parameters such as the amount of external contours, the tracking of the nozzle (raster), and the distance between rasters are usually considered default parameters, but could also be modified in order to improve surface finish,[1–12] cost,[6,13–15] and performance.[16–27]

Many authors have reported studies of the mechanical strength in FDM-built parts under static loading. All of them have come to the conclusion that anisotropy is always present in FDM parts because of the manufacturing conditions. The most studied parameters, in a static situation, have been build orientation,[16,19,22,23,25,27] raster angle,[19,21–23,25,27] raster width,[18,21,23–25] raster-to-raster air gap,[18,21,23–25] and nozzle diameter or slice height.[21,23,25,26] It has been found that the build orientation is the most influential parameter because of the filament adhesion between adjacent layers.[16,22,23,25] The second one in importance has been found to be the raster track along each layer: the more aligned the filaments are with the strain applied, the higher the strength becomes.[21,23,27]

Increasingly, parts manufactured by FDM tend to become end-use parts in applications such as machinery or

[1]Grup d'Enginyeria de Productes Industrials (GEPI) and [2]Grup d'Enginyeria de Materials (GEMAT), Institut Químic de Sarrià, Universitat Ramon Llull, Barcelona, Spain.

 MARY ANN LIEBERT, INC. • VOL. 1 NO. 2 • 2014 • DOI: 10.1089/3dp.2013.0007

transportation. In those cases, it should be taken into account that forces acting on those parts might vary in direction and extent at a given frequency. One of the major drawbacks when using parts under dynamic loading is the appearance of resonance. Such difficulty could be overcome by increasing both the stiffness/mass ratio and the damping properties of the part. Thus, understanding the influence of the building parameters affecting the stiffness or the damping factor of an FDM-produced part becomes essential.

Few studies have been carried out to characterize the dynamic mechanical behavior of FDM parts. Most of them have focused on determining properties of new materials to be used in FDM.[28–30] On the other hand, dynamic properties of acrylonitrile butadiene styrene (ABS)[31] and polycarbonate (PC)[32] FDM-produced parts have been studied running isothermal frequency sweeps between 10 and 100Hz. Parameters studied in both publications were built style, raster width, and raster angle. Built style (part interior style in Insight® FDM control software) refers to sets of parameters named as solid-normal, sparse, and sparse-double dense. Once a set has been selected, the user is able to select the amount of interior contours, the distance between rasters, and the amount of layers with fixed raster definition. Raster width refers to the width of the deposited material; this parameter depends not only on the nozzle tip diameter but also on the plastic extrusion rate because of swelling. Raster angle refers to the direction in which material is deposited with respect to the *X* direction of the building area. Both studies confirmed that process parameters affected significantly the dynamical mechanical properties of the samples.

The present work shows the results obtained for PC parts made using a Fortus 400mc FDM machine. Specimens manufactured were tested with a dynamic mechanical analysis (DMA) apparatus to evaluate the influence of the following building parameters: nozzle diameter, raster-to-raster air gap, and the amount of contours. Experiments were carried out under specific test conditions (temperature, frequency, and amplitude) in order to find whether the influence of building parameters is more significant than the test parameters under dynamic performance or not. The objective consists of determining the degree of influence of the fabrication parameters. The fact of having such knowledge would make it possible to determine specific fabrication parameters for specific applications.

DMA measures the elastic (storage modulus) and the viscous response (loss modulus) of a sample under an oscillating load. The storage modulus ($G'$) measures the maximum energy stored during one cycle of oscillation and it is related to the stiffness of the material. The loss modulus ($G''$) stands for the amount of energy dissipated by the sample. The ratio between the loss modulus and the storage modulus is known as $\tan(\delta)$ (damping factor), where $\delta$ is the phase angle between the strain and the response of the sample. The damping factor is related to the degree of molecular mobility in a polymer, which has a direct influence on the material impact resistance.[33]

Statistical design of experiments (DOE) has been applied in order to be able to obtain significant results with the minimum number of specimens. Taguchi methodology has been chosen for its robustness. Afterward, an analysis of variance (ANOVA) has been performed to detect the most significant parameters and levels that influence the dynamic performance of the specimens.

## Materials and Methods

### *Factors and Design of Experiments*

The parameter selection has been done taking into consideration the results of previous investigations concerning mechanical properties[16–27] and other additive manufacturing issues such as surface finish[1–12] and cost.[6,13–15] The selected fabrication and test factors, as well as the selected levels, are shown in Table 1.

The build parameters (Figure 1) are defined as follows:

- Tip size (A): The size of the tip determines the diameter of the extruded filament (contour and raster width) and defines the slice height. This parameter affects greatly the surface roughness and the cost of the manufactured part.

**Table 1. Fabrication and test factors considering levels for experimentation**

| Fixed factors | | | Variable factors | | | | | |
|---|---|---|---|---|---|---|---|---|
| | | | | | Level | | | |
| Factor | Value | Unit | Factor | Symbol | −1 | 0 | 1 | Unit |
| Material | Polycarbonate | — | Tip | A | T12 | T16 | T20 | — |
| Support | Basic | — | Slice height | | 0.1778 | 0.254 | 0.3302 | mm |
| Part fill style | Multiple contours | — | Contour width | | 0.3556 | 0.508 | 0.6604 | mm |
| Part interior style | Solid—normal | — | Raster width | | 0.3556 | 0.508 | 0.6604 | mm |
| Build direction | Z | — | Number of contours | B | 1 | 5 | 10 | — |
| Raster angle | 45 | ° | Raster-to-raster air gap | C | 0 | 0.25 | 0.5 | mm |
| Visible surface style | Normal | — | Amplitude | D | 20 | 40 | 60 | μm |
| Contour-to-raster air gap | 0 | mm | Temperature | E | 30 | 60 | 100 | °C |
| Contour-to-contour air gap | 0 | mm | Frequency | F | 1 | 40 | 100 | Hz |

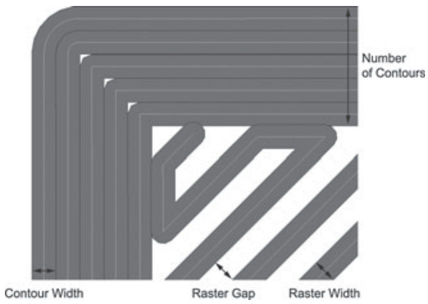


**Figure 1.** Fabrication parameter's description

- Number of contours (B): The number of perimeter trajectories to build around all outer and inner part curves. It also affects the cost of the part but not in the same degree as factor A.
- Raster-to-raster air gap (C): The raster is defined as the trajectory of the nozzle inside contours filling the interior nonvisible section of the part. The gap is the distance between two adjacent rasters in the same layer. Negative air gaps were not considered because they can degrade surface quality and dimensional tolerances.[18] This parameter affects the cost of a part. The bigger the air gap, the less material is needed, decreasing building time and the amount of material.

Amplitude, frequency, and temperature have been introduced as factors in the DOE, assuming that they may have influence on the dynamic properties of the produced parts. First, amplitude sweeps at a constant temperature have been carried out in order to establish the range of linear viscoelastic behavior. All the samples studied must be within this range to obtain consistent results. Frequency values have been set to meet industry applications; 40 and 100 Hz are usual frequencies to accomplish automotive and aeronautic specifications, respectively. Temperature levels were chosen in a high range for two reasons: to meet industrial applications and to verify that it is an important factor to be taken into account in specific applications. Since automotive parts are tested at 60°C and the usual working temperature could be 30°C, it was decided to set these two temperatures as the midlevel and lower level.

A classical DOE considering six factors evaluated with three levels for each one would require 729 ($3^6$) experiments. The Taguchi approach reduces the amount of experimental runs and still allows an in-depth understanding of process parameters and their interaction effects on FDM-built parts.[10,11] Taguchi proposes an experimental plan, in terms of orthogonal array, giving a certain combination of parameters for each experiment.

In this study, the degree of freedom is 24 since 6 factors at 3 levels and 3 interactions (A×B, B×C, and A×C) have been considered. The appropriate orthogonal array for this case is $L_{27}$. The assignment of factors and interactions has been made on the basis of a linear graph as shown in Figure 2, in order to avoid confusion between factors.

Each dot in the linear graph represents the factor column number. On the other hand, the line joining two dots corresponds to the interaction between the factors assigned to these columns. Finally, the numbers represent the column number to which these factors and interactions have been assigned. As the present investigation has been focused on studying mainly manufacturing factors and their interactions, columns 1, 2, and 5 have been assigned to factors A, B, and C, respectively. Test factors D, E, and F have been assigned to columns 9, 10, and 12. Column 13 has been assigned to the experimental error. This configuration also allows the fabrication parameters to be set in a full factorial DOE, making a detailed study on its influence possible. The final column assignation of the $L_{27}$ orthogonal matrix is as shown in Table 2.

### *Specimen Design and Fabrication*

Rectangular specimens have been designed according to material specifications and to have the maximum size supported by the dual-cantilever clamp of the DMA. Their dimensions are 60 mm × 15 mm × 3 mm. The specimens have been designed using SolidWorks® 2013 and processed for manufacturing using Insight® 8.1.1, where the building parameters were set. Three PC parts were manufactured for each experiment using the Stratasys Fortus 400 mc machine.

### *Experimental Procedure*

Three samples have been produced for each set of building factors. The experiments have been conducted with the corresponding test parameters using the DMA Q800 TA. The results obtained correspond with the average value of 50 measurements done during these experiments.

### *Statistical Analysis*

In order to determine the most influential factors in a DOE using Taguchi's method, a signal-to-noise (*S*/*N*) ratio has been defined. In the Taguchi method the term "signal" represents the desirable target and "noise" represents the undesirable value. The objective of the experimental plan is to maximize the studied properties. The *S*/*N* ratio has been calculated for each parameter level using Equation 1:

$$\eta = -10 log_{10}\left(\frac{1}{n}\sum_{i=1}^{n}\frac{1}{y_i^2}\right) \qquad (1)$$

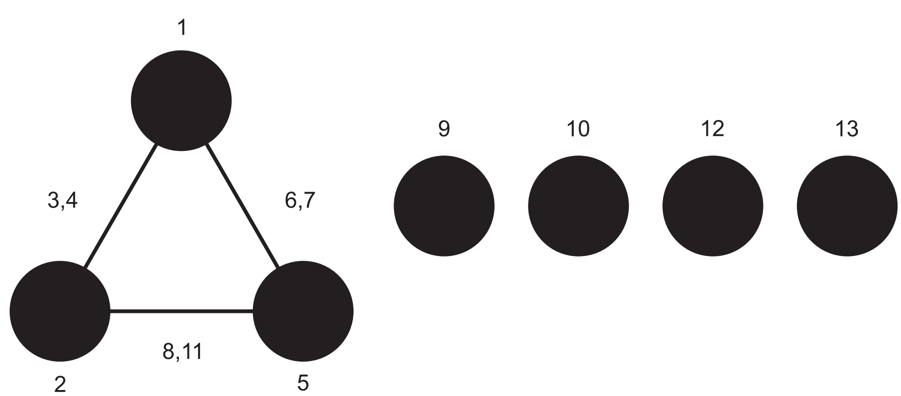


**Figure 2.** $L_{27}$ linear graph.


MARY ANN LIEBERT, INC. • VOL. 1 NO. 2 • 2014 • DOI: 10.1089/3dp.2013.0007

**Table 2. L27 matrix column assignation along with signal and noise values for storage modulus, loss modulus, tan delta, and stiffness**

| Exp. No. | Factor | | | | | | Storage modulus (MPa) | | Loss modulus (MPa) | | Tan delta | | Stiffness (N/m) | |
|---|---|---|---|---|---|---|---|---|---|---|---|---|---|---|
| | A | B | C | D | E | F | Signal | Noise | Signal | Noise | Signal | Noise | Signal | Noise |
| 1 | −1 | −1 | −1 | −1 | −1 | −1 | 4307.55 | 83.57 | 50.94 | 2.34 | 1.184E-02 | 7.608E-04 | 137304.17 | 3798.89 |
| 2 | −1 | −1 | 0 | 0 | 0 | 0 | 1503.80 | 27.58 | 8.22 | 0.33 | 5.464E-03 | 1.186E-04 | 46145.17 | 143.78 |
| 3 | −1 | −1 | 1 | 1 | 1 | 1 | 994.47 | 17.01 | 9.13 | 10.53 | 9.077E-03 | 1.036E-02 | 30946.01 | 262.39 |
| 4 | −1 | 0 | −1 | 0 | 0 | 1 | 4642.97 | 92.64 | 48.64 | 4.54 | 1.048E-02 | 1.013E-03 | 145505.78 | 1952.42 |
| 5 | −1 | 0 | 0 | 1 | 1 | −1 | 2389.43 | 60.07 | 37.10 | 3.99 | 1.550E-02 | 1.280E-03 | 72350.14 | 822.65 |
| 6 | −1 | 0 | 1 | −1 | −1 | 0 | 2349.01 | 70.51 | 16.30 | 2.41 | 6.941E-03 | 1.027E-03 | 72573.96 | 1531.46 |
| 7 | −1 | 1 | −1 | 1 | 1 | 0 | 4812.50 | 57.53 | 87.20 | 7.01 | 1.813E-02 | 1.582E-03 | 145707.88 | 2778.07 |
| 8 | −1 | 1 | 0 | −1 | −1 | 1 | 4049.65 | 50.32 | 57.87 | 13.93 | 1.428E-02 | 3.395E-03 | 121029.42 | 838.09 |
| 9 | −1 | 1 | 1 | 0 | 0 | −1 | 3414.81 | 63.70 | 55.70 | 3.06 | 1.632E-02 | 1.073E-03 | 105219.32 | 1254.42 |
| 10 | 0 | −1 | −1 | 0 | 1 | 0 | 4146.94 | 214.03 | 36.29 | 3.97 | 8.741E-03 | 6.639E-04 | 135939.13 | 1828.31 |
| 11 | 0 | −1 | 0 | 1 | −1 | 1 | 2100.89 | 74.69 | 35.81 | 14.20 | 1.691E-02 | 6.047E-03 | 70925.54 | 1957.24 |
| 12 | 0 | −1 | 1 | −1 | 0 | −1 | 1472.19 | 23.89 | 11.17 | 0.90 | 7.598E-03 | 7.303E-04 | 50575.76 | 828.78 |
| 13 | 0 | 0 | −1 | 1 | −1 | −1 | 4810.25 | 135.09 | 83.71 | 5.71 | 1.739E-02 | 7.515E-04 | 169298.30 | 741.11 |
| 14 | 0 | 0 | 0 | −1 | 0 | 0 | 3349.01 | 63.42 | 23.51 | 11.63 | 7.030E-03 | 3.519E-03 | 111889.32 | 557.69 |
| 15 | 0 | 0 | 1 | 0 | 1 | 1 | 2601.91 | 25.72 | 29.35 | 10.82 | 1.126E-02 | 4.070E-03 | 86691.02 | 463.23 |
| 16 | 0 | 1 | −1 | −1 | 0 | 1 | 5499.38 | 235.36 | 53.03 | 10.00 | 9.643E-03 | 1.805E-03 | 184319.68 | 5961.83 |
| 17 | 0 | 1 | 0 | 0 | 1 | −1 | 4119.98 | 254.23 | 67.37 | 4.09 | 1.639E-02 | 1.384E-03 | 140974.13 | 4304.66 |
| 18 | 0 | 1 | 1 | 1 | −1 | 0 | 4844.85 | 169.81 | 134.26 | 2.43 | 2.772E-02 | 6.485E-04 | 155951.75 | 2992.16 |
| 19 | 1 | −1 | −1 | 1 | 0 | 1 | 4687.27 | 93.84 | 62.05 | 8.12 | 1.325E-02 | 1.859E-03 | 206276.92 | 3479.37 |
| 20 | 1 | −1 | 0 | −1 | 1 | −1 | 2068.57 | 41.09 | 18.51 | 0.63 | 8.949E-03 | 3.358E-04 | 87157.38 | 2379.04 |
| 21 | 1 | −1 | 1 | 0 | −1 | 0 | 1898.95 | 34.33 | 20.37 | 3.30 | 1.071E-02 | 1.613E-03 | 78919.83 | 2037.76 |
| 22 | 1 | 0 | −1 | −1 | 1 | 0 | 4801.88 | 86.22 | 28.23 | 1.12 | 5.881E-03 | 2.702E-04 | 203678.65 | 1049.33 |
| 23 | 1 | 0 | 0 | 0 | −1 | 1 | 3808.77 | 71.73 | 56.12 | 19.95 | 1.480E-02 | 5.544E-03 | 160916.13 | 1067.33 |
| 24 | 1 | 0 | 1 | 1 | 0 | −1 | 3398.84 | 47.86 | 63.08 | 7.45 | 1.858E-02 | 2.375E-03 | 136557.13 | 558.07 |
| 25 | 1 | 1 | −1 | 0 | −1 | −1 | 5252.58 | 142.59 | 75.70 | 7.93 | 1.444E-02 | 1.841E-03 | 226104.70 | 6657.85 |
| 26 | 1 | 1 | 0 | 1 | 0 | 0 | 5350.96 | 104.12 | 107.71 | 4.80 | 2.014E-02 | 1.252E-03 | 216505.57 | 2079.09 |
| 27 | 1 | 1 | 1 | −1 | 1 | 1 | 5162.55 | 27.61 | 36.92 | 3.54 | 7.151E-03 | 6.514E-04 | 205212.97 | 1508.72 |

where $\eta$ is the average $S/N$ ratio, $n$ is the number of experiments conducted at level $i$, and $y_i$ is the measured value of the property. Larger values of $S/N$ ratio are desirable as a larger $S/N$ ratio results in smaller product variance around the target value. Thus, the levels with maximum $S/N$ ratio are considered optimal. Optimizing the $S/N$ ratio would define the optimal factors if there would be linear dependency between the signal and the $S/N$ ratio and the standard deviation and the $S/N$ ratio. On the other hand, if there is no correlation, or it is not the same for the signal and the noise, a dual-response approach is needed: find the factors that maximize the signal response and minimize the noise.

An ANOVA has been performed using the signal and noise values obtaining the influence of each parameter in all dynamic properties studied. The parameters that showed an influence lower than 10% have been considered not significant. The effect of the levels for each parameter on signal and noise has been then studied in order to find the influence of the different levels on the response.

## Results

The signal and noise values obtained for each property are shown in Table 2. Results showed that the elastic behavior (storage modulus and stiffness) of the samples was not influenced by the testing parameters, while the viscous behavior [loss modulus and tan($\delta$)] did. The results obtained did not present linear dependency between the $S/N$ ratio and the signal or the noise; thus, a dual-response analysis was made for a better understanding of the influence of the parameters. Table 3 exhibits the significance of factors, and the levels in which the signal is higher and noise lower.

Figure 3 shows the effect of the levels of factors on the properties signal studied. The number of contours followed by the raster air gap appears to be the most influential parameters on the storage modulus value. The maximum $G'$ is

| Table 3. Optimum factor level with significant factors and interactions in order | | | | | | | | |
|---|---|---|---|---|---|---|---|---|
| | Storage modulus | | Loss modulus | | Tan delta | | Stiffness | |
| Factor | Signal | Noise | Signal | Noise | Signal | Noise | Signal | Noise |
| A | 3 | 1 | 2 | 1 | 2 | 3 | 3 | 1 |
| B | 3 | 1 | 3 | 1 | 3 | 3 | 3 | 2 |
| C | 1 | 3 | 1 | 3 | 2 | 1 | 1 | 3 |
| D | 3 | 1 | 3 | 1 | 3 | 1 | 3 | 3 |
| E | 1 | 2 | 1 | 3 | 1 | 2 | 2 | 3 |
| F | 3 | 3 | 1 | 1 | 1 | 1 | 3 | 2 |
| Significant | B, C | A, C, B | B, D | F, C | D, B, E | F, C, D | C, B, A | B, C |

obtained when the number of contours is the highest and there is no air gap. $G''$ value is also influenced greatly by the number of contours. The higher the number of contours, the higher $G''$ becomes.

Amplitude plays an important role in the loss modulus and consequently in the tan($\delta$); the higher the amplitude, the higher $G''$ and tan($\delta$). Tan($\delta$) is also influenced by the number of contours and the temperature. The response increases as the number of contours is the maximum and the temperature the lowest. Stiffness is affected only by building parameters, where the number of contours is the most influent, followed by the raster air gap and the nozzle diameter. The highest stiffness is observed when the number of contours and the nozzle diameter are in the top level and the raster air gap in the bottom level.

The influence of the factor levels on the variability of the signal is shown in Figure 4. The lowest variation of the storage modulus has been obtained when using the smallest nozzle diameter, the minimum number of contours, and the biggest distance between rasters. Testing frequency affects the loss modulus noise. The distance between rasters also affects the loss modulus noise but in a less extend. The higher the distance between raster and the lower the applied frequency, the smaller the product variance around the loss modulus signal. As expected, the damping factor variability is significantly affected by the frequency. Raster gap and amplitude also affect the variability but almost in the limit of being ruled out. The smallest noise is achieved when the frequency is the maximum and when the distance between rasters and the amplitude are the lowest. Building parameters are the only ones affecting the noise of the stiffness. The signal varies less when five contours are used to build the sample (midlevel) and the air gap is the maximum.

A dual-response approach had to be done in the interest of solving contradictions between factor levels. Both the number of contours and the raster air gap affected the signal and noise. The influence of the number of contours on the signal has been more significant than that on the noise.

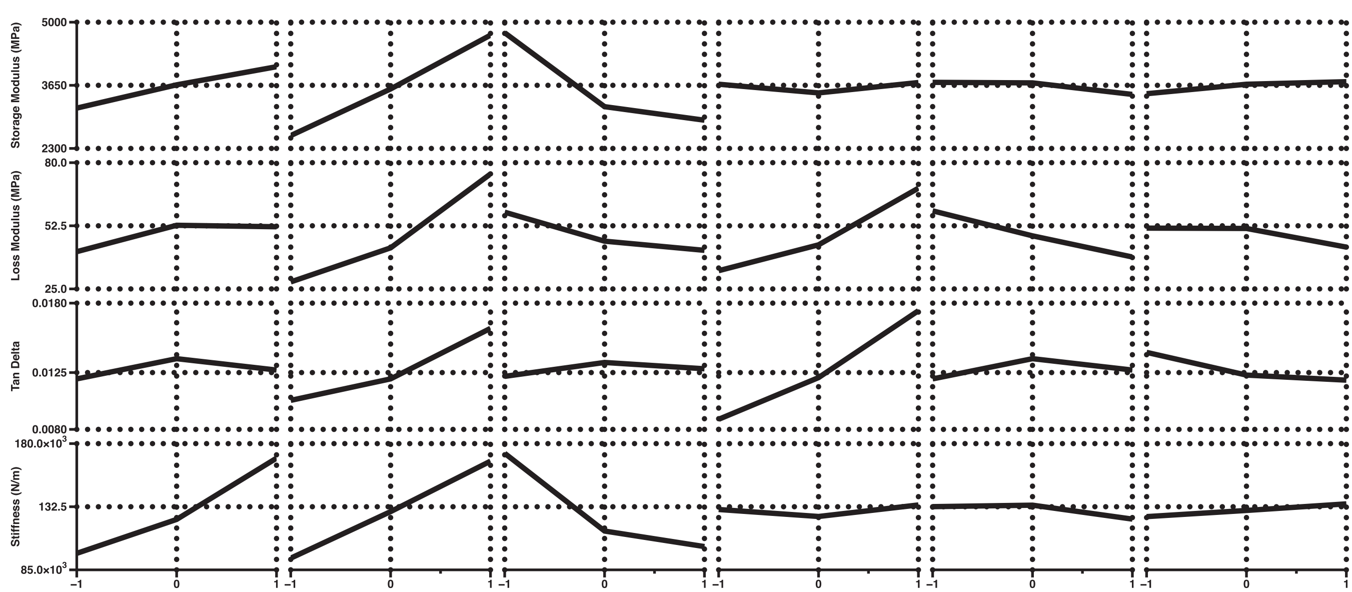


**Figure 3.** Plot for factor effect on signal; columns represent factors from A to F, and rows represent properties.


MARY ANN LIEBERT, INC. • VOL. 1 NO. 2 • 2014 • DOI: 10.1089/3dp.2013.0007

Therefore, in order to obtain the highest modulus, to build the maximum number of contours seems to be the most adequate. A similar trend has been detected regarding the gap between rasters. In this case, the gap has been set at zero to obtain the highest modulus.

Loss modulus did not present contradictions between the levels and factors affecting both signal and noise. Regarding loss modulus, the parameters for best results have been set at 10 contours and the maximum gap. Loss modulus is affected by the test parameters: amplitude and frequency. Higher amplitudes and lower frequencies maximize the signal, while reduce the variability.

Both build and test parameters affect significantly tan($\delta$). The best combination is found when the number of contours is the maximum and the distance between rasters is the minimum. The temperature, frequency, and the amplitude of the oscillation also affect the damping factor. Lower temperatures and frequencies give rise to a lower tan($\delta$). Amplitude affects both signal and noise.

On the other hand, stiffness is affected only by fabrication parameters. The viscoelastic behavior of the sample is affected: first, by the raster air gap; second, by the number of contours; and finally, by the nozzle diameter. The most influential parameter in the variance of the signal is the number of contours followed by the distance between rasters. Since a contradiction between level factors has been found, a further study would be required to get more insight in this phenomenon.

In order to maximize the signal, the nozzle diameter should be the widest possible, the number of contours the maximum, and there should be no air gap between rasters. The minimum variance is found when the contours are at the midlevel and the distance between rasters is the maximum. Since the diameter of the nozzle does not affect the variability, its selection should be considered only to maximize the stiffness, so the nozzle diameter should be wider.

The other two fabrication parameters affect the signal and the noise likewise. Experiments 22, 24, 25, and 26 (Table 2) present all the possible combinations with these factors and levels. Experiment 24 presents the lowest signal and noise; experiment 25 presents the opposite, so both of them are dismissed. Experiments 22 and 26 present the best $S/N$ ratio. Number 26 shows higher signal than 22, but its variation is also higher. In order to obtain the highest signal with less variation, the best experiment is 22.

## Discussion

The results obtained have shown that the building factors were the only ones affecting the elastic response of the PC FDM-produced parts. On the other hand, the influence of test parameters on the viscous behavior of the parts was also important and will be discussed separately.

Storage modulus represents the elastic part of the mechanical behavior. It should be noted at this point that using a smaller nozzle diameter implies a smaller slice height and contour and raster width. Layer height affects the interlayer bonding, while the contour and raster width affect mainly the bonding quality between filaments in the same slice. The number of slices determines the temperature gradient toward the bottom layers; the more slices, the bigger the temperature gradient. Thus, in order to obtain a maximum elastic behavior, the nozzle should be wider.

A weak interlayer bonding is responsible for the decrease in strength because distortion occurs with high temperature gradient toward the bottom layers. As the layer thickness increases, less number of layers will be required, distortion effect is minimized, and strength increases.[23]

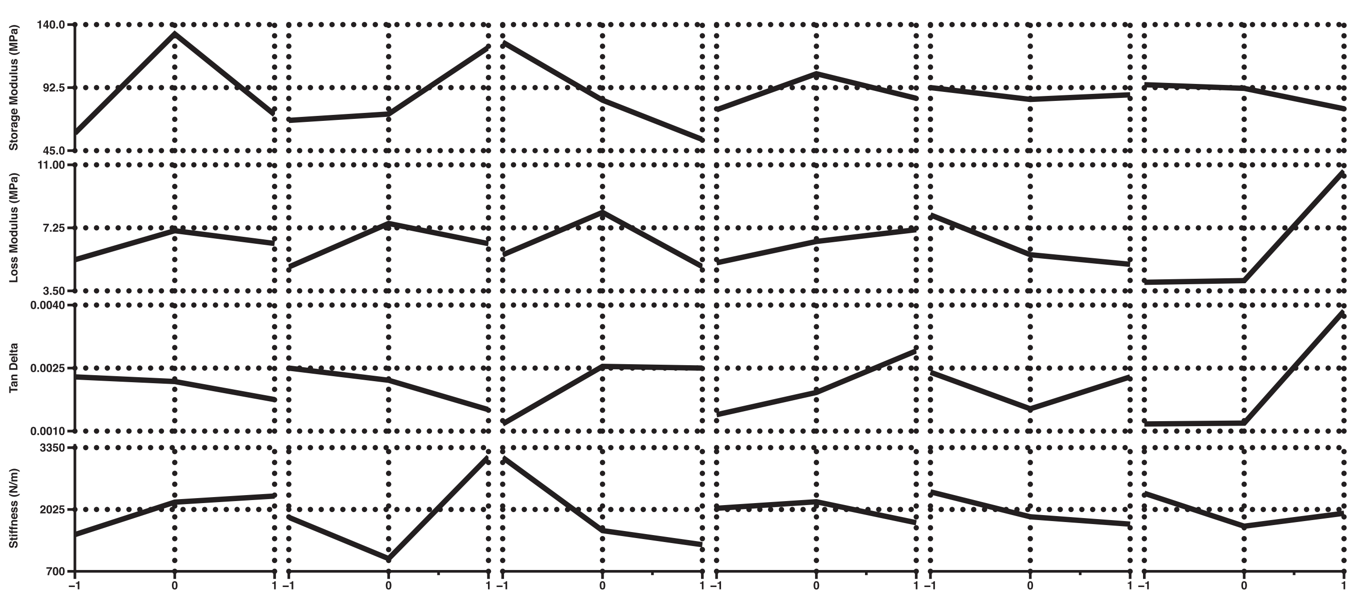


**Figure 4.** Plot for factor effect on noise; columns represent factors from A to F, and rows represent properties.

On the other hand, if the diameter of the extruded filament is smaller, the temperature gradient between its inner and outer part is smaller; consequently, the bonding quality between filaments in the same layer is better. As a result of this, the storage modulus becomes greater. This apparent contradiction shows why parameter A was not of significance.

When bonding between layers is not good because of the slice height, bonding between extruded filaments on the same layer is better and vice versa. The contours act like reinforcement fibers because the direction of fabrication is related to how the sample is deformed. Subsequently, it has sense to consider that more contours mean a more elastic sample. Minimum raster-to-raster air gap makes the inside of the part more continuous (with fewer voids). Thus, the specimen becomes able to readily return to its normal state after deformation.

Maximum number of contours and no air gap mean more amount of material used. Still, it has to be taken into account that this combination of factors makes the manufacture procedure more expensive.

The size of the nozzle is the most significant factor in cost. Using a smaller tip means that the profile error would be the minimum.[10] However, larger amount of material and longer time are consumed, resulting in a bigger cost of production.

The loss modulus of a PC FDM-produced part cannot be controlled only by fabrication parameters since the amplitude of the strain and the frequency affect its viscous behavior. Taken into account this fact, it can be stated that building parameters have a significant impact on the $G''$: a maximum number of contours and a maximum distance between rasters increase the value and reduce $G''$ variability. As it has been stated previously, the contours seem to act like reinforcement fibers and the distance between interior filaments (set as maximum) makes the part more flexible, and consequently its ability to absorb shocks increases. This combination of fabrication parameters makes the manufacturing cost lower since the raster air gap is one of the main parameters influencing the amount of material used and the building time.

The same situation is presented when dealing with $\tan(\delta)$. Fabrication and test parameters affect the damping factor. Amplitude, frequency, and temperature play an important role in the molecular energy dispersion mechanism. The number of contours, as should be expected, has the same effect as with storage modulus and loss modulus. When there is no air gap in the raster, $\tan(\delta)$ becomes less variable. Such a combination of parameters makes building the part more expensive since there is no air gap between rasters; thus, more material and building time are needed.

Stiffness is, like the storage modulus, only affected by fabrication parameters. The difference is that the nozzle diameter influences the rigidity of the specimen. The bigger the diameter is, the better results are obtained. As expected, the bonding quality affects storage modulus and stiffness in the same way. The reason why the best performance overall is obtained when the number of contours is set in its middle level is its combination with the other building factors. A combination of a wider nozzle and raster width with a large number of contours takes almost all the inner space of the part. Consequently, it is built mainly with contours leaving less space for inner rasters among contours, sample becomes more solid, and stiffness increases. When using the widest tip, the amount of material required and the building time decrease, thus reducing the manufacturing costs.

## Conclusions

In the present article the dynamic mechanical properties of PC parts manufactured via an FDM process have been analyzed on the basis of building and test parameters. Samples have been built varying nozzle diameter, number of contours, and the distance between rasters. Tests have been carried out using different experimental range of amplitude, frequency, and temperature. The results obtained confirmed that dynamical properties studied depend on the building and test parameters. Building parameters can control the elastic behavior of the manufactured parts by FDM. In that case, test conditions did not affect significantly in comparison with the building parameters. On the other hand, testing parameters showed a great influence on the damping capacity of the manufactured parts.

The number of contours is the most influential parameter overall since it affects all the properties (elastic and viscous) analyzed. All the properties evaluated become optimum when the amount of contours is the maximum. Contours strengthen the part causing an increased elastic behavior. Its influence on the manufacturing cost is not as important as other fabrication parameters; thus, it is an interesting approach in order to strengthen the parts without compromising the cost.

Selecting the right building parameters has been revealed as a complex task; this complexity increases even more when cost, dimensional accuracy, and surface finish are considered. The effect of various factors and their interactions is difficult to explain, but some generalization has been found. Improvement of the elasticity or the stiffness of a part is presented when the parts are manufactured as continuous as possible and also when the direction of filaments is important to make them act as reinforcements.

Further studies are needed to understand the influence of the parameters studied on the dynamic mechanical properties of FDM-produced parts. However, the results obtained with the present work are expected to be similar for other plastic materials used in FDM. The value of the property under consideration may probably change, but not how different factors and levels affect the dynamic behavior.

## Acknowledgments

M.D.-E. was supported by an IQS fellowship. Part of this work was supported by SGR 2009 Grant to Grup d'Enginyeria de materials (GEMAT) from Generalitat de Catalunya and a

Grant from the Catalan Agency for Enterprise Support (ACC1Ó).

## Author Disclosure Statement

No competing financial interests exist.

### References

1. Masood SH, Rattanawong W, Iovenitti P. Part build orientations based on volumetric error in fused deposition modelling. Int J Adv Manuf Technol 2000;16:162–168.
2. Anitha R, Arunachalam S, Radhakrishnan P. Critical parameters influencing the quality of prototypes in fused deposition modelling. J Mater Process Technol 2001;118:2–5.
3. Campbell RI, Martorelli M, Lee HS. Surface roughness visualisation for rapid prototyping models. Comput Des 2002; 34:717–725.
4. Pérez C. Analysis of the surface roughness and dimensional accuracy capability of fused deposition modelling processes. Int J Prod Res 2002;40:2865–2881.
5. Armillotta A. Assessment of surface quality on textured FDM prototypes. Rapid Prototyp J 2006;12:35–41.
6. Byun H-S, Lee KH. Determination of the optimal build direction for different rapid prototyping processes using multi-criterion decision making. Robot Comput Integr Manuf 2006;22:69–80.
7. Ahn D, Kweon J-H, Kwon S, et al. Representation of surface roughness in fused deposition modeling. J Mater Process Technol 2009;209:5593–5600.
8. Vijay P, Danaiah P, Rajesh KVD. Critical parameters effecting the rapid prototyping surface finish. J Mech Eng Autom 2012;1:17–20.
9. Boschetto A. 3D roughness profile model in fused deposition modelling. Rapid Prototyp J 2013;19:240–252.
10. Sood AK, Ohdar RK, Mahapatra SS. Improving dimensional accuracy of fused deposition modelling processed part using grey Taguchi method. Mater Des 2009;30:4243–4252.
11. Equbal A, Ohdar RK, Mahapatra SS. Prediction of dimensional accuracy in fused deposition modelling: a fuzzy logic approach. Int J Prod Qual Manag 2011; 7:22–43.
12. Pérez CJL. Analysis of the surface roughness and dimensional accuracy capability of fused deposition modelling processes. Int J Prod Res 2002;40:2865–2881.
13. Thrimurthulu K, Pandey PM, Venkata Reddy N. Optimum part deposition orientation in fused deposition modeling. Int J Mach Tools Manuf 2004;44:585–594.
14. Alexander P, Allen S, Dutta D. Part orientation and build cost determination in layered manufacturing. Comput Des 1998;30:343–356.
15. Xu F, Loh H, Wong Y. Considerations and selection of optimal orientation for different rapid prototyping systems. Rapid Prototyp J 1999;5:54–60.
16. Foyos J, Noorani R, Mendelson M, et al. Effect of layer orientation on mechanical properties of rapid prototyped samples. Mater Manuf Process 2000;15:107–122.
17. Rodríguez J. Mechanical behavior of acrylonitrile butadiene styrene (ABS) fused deposition materials. Experimental investigation. Rapid Prototyp J 2001; 7:148–158.
18. Ahn SH, Montero M, Odell D, et al. Anisotropic material properties of fused deposition modeling ABS. Rapid Prototyp J 2002;8:248–257.
19. Bellini A, Güçeri S. Mechanical characterization of parts fabricated using fused deposition modeling. Rapid Prototyp J 2003;9:252–264.
20. Rodríguez JF, Thomas JP, Renaud JE. Mechanical behavior of acrylonitrile butadiene styrene fused deposition materials modeling. Rapid Prototyp J 2003;9:219–230.
21. Lee BH, Abdullah J, Khan Za. Optimization of rapid prototyping parameters for production of flexible ABS object. J Mater Process Technol 2005;169:54–61.
22. Lee CS, Kim SG, Kim HJ, et al. Measurement of anisotropic compressive strength of rapid prototyping parts. J Mater Process Technol 2007;187–188: 627–630.
23. Sood AK, Ohdar RK, Mahapatra SS. Parametric appraisal of mechanical property of fused deposition modelling processed parts. Mater Des 2010;31:287–295.
24. Bagsik A. Mechanical properties of fused desposition modeling parts manufactured with ULTEM 9085. In: ANTEC 2011 Plastics: Annual Technical Conference Proceedings, 2011, Boston, MA. Curran Associates, Inc., Red Hook, NY, 2011; pp. 1294–1298.
25. Sood AK, Ohdar RK, Mahapatra SS. Experimental investigation and empirical modelling of FDM process for compressive strength improvement. J Adv Res 2012;3:81–90.
26. Domingos M, Chiellini F, Gloria A, et al. Effect of process parameters on the morphological and mechanical properties of 3D Bioextruded poly(E-caprolactone) scaffolds. Rapid Prototyp J 2012;18:56–67.
27. Ziemian C, Sharma M, Ziemian S. Anisotropic mechanical properties of ABS parts fabricated by fused deposition modelling. In: Gokcek M, ed. Mechanical Engineering. Intech, 2012; pp. 159–180.
28. Shofner M. Nanofiber-reinforced polymers prepared by fused deposition modeling. J Appl Polym Sci 2003;89: 3081–3090.
29. Nikzad M, Masood SH, Sbarski I. Thermo-mechanical properties of a highly filled polymeric composites for fused deposition modeling. Mater Des 2011;32:3448–3456.
30. Sa'ude N, Masood S, Nikzad M, et al. Dynamic mechanical properties of copper-ABS composites for FDM feedstock. Int J Eng Res Appl 2013;3: 1257–1263.
31. Arivazhagan A, Masood SH. Dynamic mechanical properties of ABS material processed by fused deposition modelling. Int J Eng Res Appl 2012;2: 2009–2014.
32. Arivazhagan A, Masood SH, Sbarski I. Dynamic mechanical analysis of fused deposition modelling processed polycarboante. ANTEC 2011 Plastics: Annual Technical Conference Proceedings, 2011, Boston, MA. Curran Associates, Inc., Red Hook, NY, 2011; pp. 950–955.
33. Menard K. Dynamic Mechanical Analysis: A Practical Introduction (1 edition March 25, 1999). CRC Press, New York, NY, 2008.

Address correspondence to:
*Guillermo Reyes*
*Grup d'Enginyeria de Productes Industrials (GEPI)*
*IQS, Universitat Ramon Llull*
*Via Augusta, 390*
*Barcelona 08017*
*Spain*

*E-mail:* guillermo.reyes@iqs.url.edu